World Academy of Science, Engineering and Technology
International Journal of Mechanical and Mechatronics Engineering
Vol:10, No:10, 2016

The Simulation and Experimental Investigation to Study the Strain Distribution Pattern during the Closed Die Forging Process

D. B. Gohil

***Abstract*—**Closed die forging is a very complex process, and measurement of actual forces for real material is difficult and time consuming. Hence, the modelling technique has taken the advantage of carrying out the experimentation with the proper model material which needs lesser forces and relatively low temperature. The results of experiments on the model material then may be correlated with the actual material by using the theory of similarity. There are several methods available to resolve the complexity involved in the closed die forging process. Finite Element Method (FEM) and Finite Difference Method (FDM) are relatively difficult as compared to the slab method. The slab method is very popular and very widely used by the people working on shop floor because it is relatively easy to apply and reasonably accurate for most of the common forging load requirement computations.

***Keywords*—**Experimentation, forging, process modeling, strain distribution.

I. Introduction

CLOSED die forging is the term applied to all forging operations involving three-dimensional shape control. It is an extremely complex forming process of deformation mechanics. In the closed die forging process, the material flow is found to be non-steady state and non-uniform in the die cavity, the friction at the die-billet interface is also reasonably high, and the heat transfer between the deforming material and die is also very complicated. All of these complexities pose really a challenging situation for evaluation.

Most people involved in metal forming face with the problem of forming load estimation. In majority of the cases, there are three commonly adopted methods:

a) Analytical Method: In this method, a job to be manufactured by forging is divided into several zones. Forces and stresses are calculated for every zone and then summed up to get the total amount of forging load and value of stresses. The approximate theory which is most widely used for the analytical predictions is also known as the slab method.

b) Empirical Formulae: Empirical equations which are developed based on experience can also be implemented by using the flow stress of the material and according to the complexity of Job.

c) Field Experience: The field experience which may be useful to estimate the forging load requirements for new component is based on the data available for the similar kind of components manufactured by the forging process previously.

The present work is an attempt of analyzing a problem related to the closed die forging by using a slab method.

II. Forging Process Modelling

The modeling and simulation of closed die forging process has been carried out by using analytical and numerical methods [1], [11]. For the purpose of simulation, a billet having half cylindrical shape billet with appropriate H/D ratio, has been deformed between two die halves as shown in Fig. 1. The deformation process before flash formation and after flash formation has been depicted in Figs. 2 and 3, respectively.

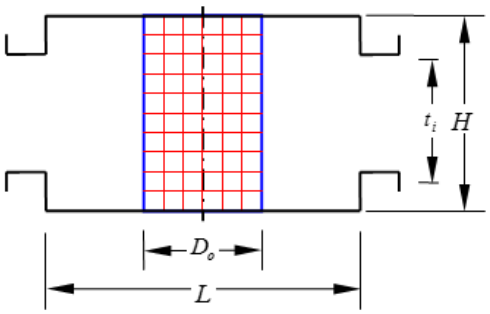

Fig. 1 Initial configuration of Die-Billet geometry

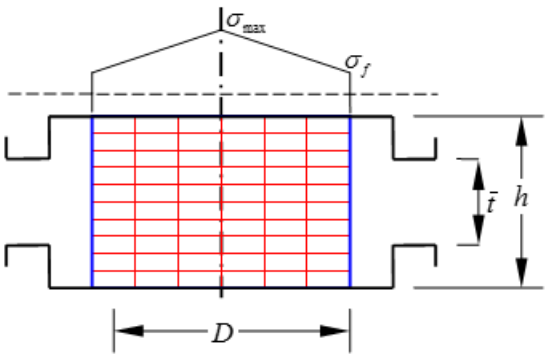

Fig. 2 Die-Billet geometry during upsetting process

Fig. 1 represents the die-billet configuration in the beginning of the closed die forging process. The billet is

D. B. Gohil is Associate Professor in Mechanical Eng. Dept. of the Sardar Vallabhbhai National Institute of Technology, Surat, 395007 India (phone: +91-261-2201991; fax: +91-261-2228394; e-mail: dbg@med.svnit.ac.in).

shown with the help of a blue color, while the square grid marking has been shown in red color.

Fig. 2 shows the die-billet configuration during upsetting process presuming the ideal conditions because of which the shape of the square grid changes to rectangular one. However, it should be noted that in actual upsetting, some amount of bulging is always observed which depends upon the frictional conditions prevailing between the contact surfaces of die and billet.

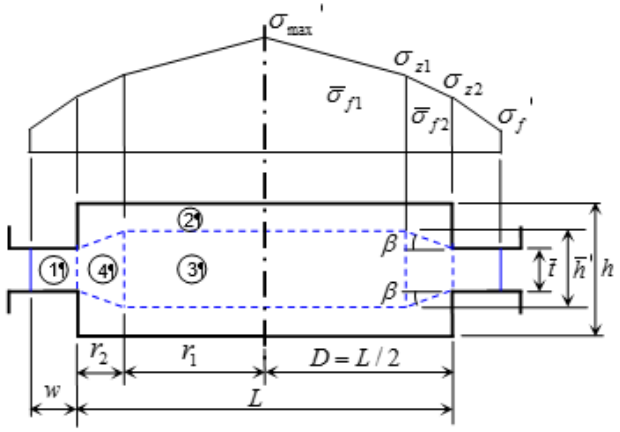

Fig. 3 Die-Billet geometry during Flash formation process

Fig. 3 depicts the die-billet geometry during the flash formation which occurs at the end of the close die forging process. At the end of the process, the material is assumed to flow in to flash by shearing along the surface indicated by dashed line in Fig. 3. Zone 1 (encircled digit 1) indicates a flash zone. The material in zone 2 (encircled digit 2) does not flow further even if there is a downward movement of the upper die half. The downward movement of the upper die half causes the movement of the work material from zone 3 to zone 4 and then ultimately to zone 1.

A. Estimation of the Flow Stress

Forging is a deformation process which involves several variables interrelated by more or less complex functions. The method discussed here is used to simulate the hot die forging process to calculate the flow stress, maximum stress, strain before flash formation, strain in flash, load, temperatures of die and billet. The flow stress relationship has been implemented as a subroutine in the algorithm [2], [12], [14].

$$\sigma_f = C\dot{\varepsilon}^m \tag{1}$$

where, $C = f(\varepsilon, T)$

The parameters C and m can be obtained from any material property hand book for different billet materials used in various types of forming processes.

B. Calculation of Strain

The strains in the die cavity as well as in the flash during different stages could be calculated as [4]:

The strain before flash formation, as shown in Fig. 2, could be computed as,

$$\varepsilon = \ln(H/h) \tag{2}$$

During flash formation, as depicted in Fig. 3, the strain in flash, indicated as encircled 1 (zone 1), may be calculated as,

$$\varepsilon_1 = \varepsilon_{tc} + \ln(\bar{t}_c/\bar{t}) \tag{3}$$

At the end of the process, the material into the flash is assumed to flow along the surface indicated by dashed line in Fig. 3. Therefore, the strain in zone 2, shown as encircled digit 2 (zone 2), i.e. ε_2 is equal to ε_{tc} which is the zone between the shearing line and the die, and the strain in zone 3 denoted by encircled digit 3, ε_3 may be computed as,

$$\varepsilon_3 = \varepsilon_{tc} + \ln(\bar{h}_c/\bar{h}) \tag{4}$$

$$\bar{h} = 0.8\bar{t}(L/2\bar{t})^{0.92} \tag{5}$$

The mean height of the convergence region 4 indicated by encircled digit 4 in Fig. 3 could be calculated as,

$$\bar{h}_1 = (\bar{h} + \bar{t})/2 \tag{6}$$

The strain in the convergence region 4 may be obtained as,

$$\varepsilon_4 = \varepsilon_{tc} + \ln(\bar{h}_c/\bar{h}_1) \tag{7}$$

C. Calculation of Strain Rates

The strain rates for the various stages of closed die forging may be calculated as follows:

Deformation process before flash formation as shown in Fig. 2 may be computed as,

$$\dot{\varepsilon} = v/h \tag{8}$$

Deformation process after Flash formation as depicted in Fig. 3 may be evaluated as,

$$\dot{\varepsilon}_1 = v/\bar{t} \tag{9}$$

$$\dot{\varepsilon}_3 = v/\bar{h} \tag{10}$$

$$\dot{\varepsilon}_4 = v/\bar{h}_1 \tag{11}$$

D. Calculation of Stresses

The stress before flash formation as shown in Fig. 2 may be computed as,

$$\sigma_{max} = \sigma_f(1 + (\mu_1 D/h)) \tag{12}$$

The stresses after flash formation as represented in Fig. 3 could be calculated as,

$$\sigma_{z2} = 2\mu_1\sigma_f(w/\bar{t}) + \sigma_f) \quad (13)$$

$$\sigma_{z1} = (K_2/K_1)\ln(\bar{t}/K_3 + K_2 r_2)) + \sigma_{z2} \quad (14)$$

$$\sigma_{\max} = ((2\mu\sigma_{f1} r_1)/h) + \sigma_{z1} \quad (15)$$

where,

$$K_1 = -2\tan\beta \quad (16)$$

$$K_2 = -\sigma_{f2}K_1 + 2\mu_2\sigma_{f2}(1+\tan^2\beta) \quad (17)$$

$$K_3 = \bar{h} - r_2 K_1 \quad (18)$$

$$\tan\beta = [1 - \{((\bar{h}/\bar{t}) - 1)/((\bar{h}/\bar{t})\ln(\bar{h}/\bar{t}))\}]^{1/2} \quad (19)$$

E. Calculation of Forces

The force required for deformation process before flash formation for the geometry as shown in Fig. 2 could be,

$$F = 2\pi\sigma_f[(h^2/4\mu_1^2)(\exp(D/h) - 1) - hD/4\mu_1)] \quad (20)$$

The force required for deformation process after flash formation for the geometry as shown in Fig. 3 would be,

$$F = F_1 + F_2 \quad (21)$$

$$F_1 = 2\pi\sigma_{z1}[(\bar{h}^2/4\mu_2^2)(\exp(\mu_2 L/\bar{h}) - 1) - \bar{h}L/4\mu_2)] \quad (22)$$

where,

$$F_2 = \sigma_f(\pi/4)(2Lw + w^2)(1 + (\mu_1 w/3\bar{t})) \quad (23)$$

F_1 is the average force on the billet, and F_2 is the average force on the flash land.

F. Calculation of Die and Billet Temperatures

The temperatures within the die cavity and in the flash during the process is calculated separately [1], [15].

G. Die cavity

The analysis for the temperature distribution for a system comprising of die-lubricant-billet may be summarized in non-dimensional form as given below.

The time has been transformed in to a non-dimensional parameter N_θ as

$$N_\theta = \alpha\theta/H^2 \quad (24)$$

$$\alpha = \lambda/\rho C_P \quad (25)$$

$$FS_{Die} = (T_D - T_{DO})/(T_{BO} - T_{DO}) \quad (26)$$

$$FS_{Billet} = (T_{BO} - T_B)/(T_{BO} - T_{DO}) \quad (27)$$

The FS_{Die} and FS_{Billet} are the two non-dimensional functions which represent the change in temperature at different locations within the die and the billet.

The change in temperature with time could be calculated as:

$$T_D = T_{DO} + FS_{Die}(T_{BO} - T_{DO}) \quad (28)$$

$$T_B = T_{BO} - FS_{Billet}(T_{BO} - T_{DO}) \quad (29)$$

The temperature rise due deformation may be estimated as,

$$\Delta T = \int(\sigma_f/\rho\, C_p)\, d\varepsilon \quad (30)$$

The heat developed during deformation gets partially transferred to the die, which may be calculated as,

$$T_{Bd} = \Delta T\ \exp(-\alpha_T\ t/\rho\ C_p\ h) \quad (31)$$

The final billet temperature may be given by,

$$T_{Bf} = T_B + T_{BD} \quad (32)$$

H. Flash Land

Due to the relatively lesser thickness of the flash in comparison with the die cavity, the temperature gradient may be neglected [3]. Thus, the average flash temperature may be calculated as,

$$T = T_{DC} + (T_{BC} - T_{DC})\ \exp(-\alpha_T(t - t_{cont})/\rho\ C_p\ \bar{t}) \quad (33)$$

The final flash temperature is therefore,

$$T_F = T + \Delta T \quad (35)$$

III. Algorithm for Simulation

A computer simulation algorithm has been developed consisting of two different loops for the two stages of forging process, viz. deformation process before flash formation and deformation process after flash formation. For the process simulation, initially the material needs to be selected from the material database [5], [8].

Then the die parameters, billet parameters, number of stages of deformation are provided. After that, the algorithm starts the computations and simulation [9], [10].

The simulation gives the output results step by step for flow stress, height, diameter, billet temperature, die temperature, strain, strain rate, and load requirement. At the end of the simulation, the computer algorithm asks for any modifications. If any, dimensions or material may be changed for the next set of computations and simulation [6], [7], [13].

The application of this computer simulation method could be applied for more complicated component as shown in Fig. 4 which depicts a connecting rod of an internal combustion

engine used in automobiles. The closed die forging process is used to manufacture the connecting rod as well as many other parts of automobiles [6], [13].

Fig. 4 Connecting rod of an internal combustion engine

IV. Experimentation

To study the closed die forging process, testing of properties was carried out on the various types of waxes commonly available in the market, and then, Paraffin wax was chosen as a model material. Because of the symmetry, only half of the geometry was studied. The half cylindrical billets of H/D ratio as 0.8, 1.0, 1.4, and 1.9 were pressurized in the closed die up till the final flash thicknesses of 5 mm, 4 mm, 3 mm, and 2 mm were obtained for all specimens. Fine graphite powder was used as a lubricant to eliminate the friction between the die and model material. The flat symmetrical surface was constrained with the help of thick glass plate to facilitate the photography of the grid pattern periodically during the course of deformation which was analyzed under the traveling microscope to measure the deformed grid size. The strain at the center of each grid was calculated and represented in a 3-D graphical form.

V. Results and Discussion

To understand the grid deformation pattern and the amount of actual strain, the entire forging process was divided in to six stages. The strain distribution pattern after each stage has been represented in 3-D graphical form in Figs. 5-10.

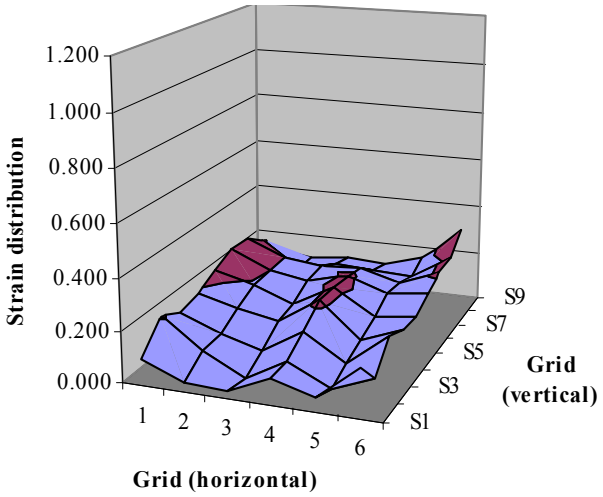

Fig. 5 Actual strain distribution pattern observed due to deformation of grid at the end of Stage 1

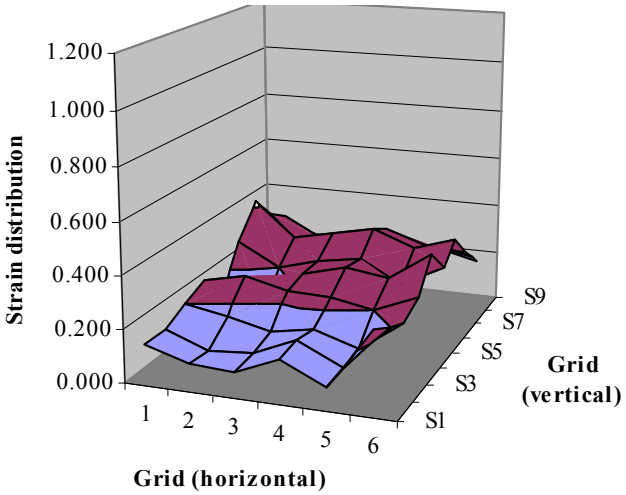

Fig. 6 Actual strain distribution pattern observed due to deformation of grid at the end of Stage 2

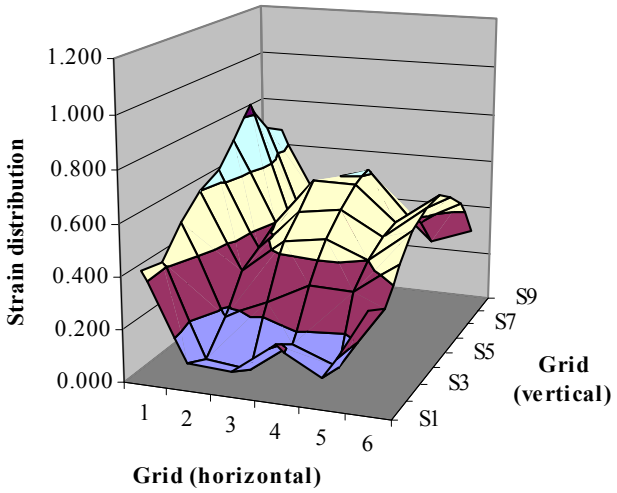

Fig. 7 Actual strain distribution pattern observed due to deformation of grid at the end of Stage 3

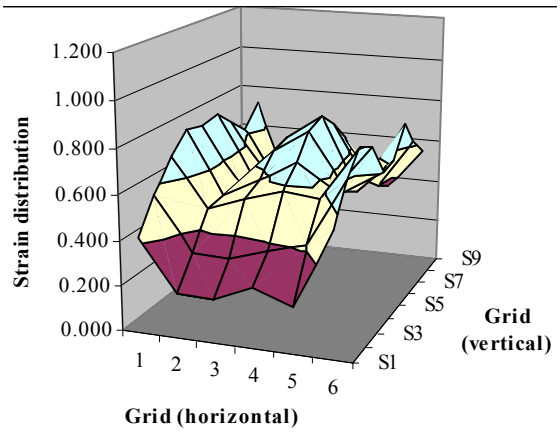

Fig. 8 Actual strain distribution pattern observed due to deformation of grid at the end of Stage 4

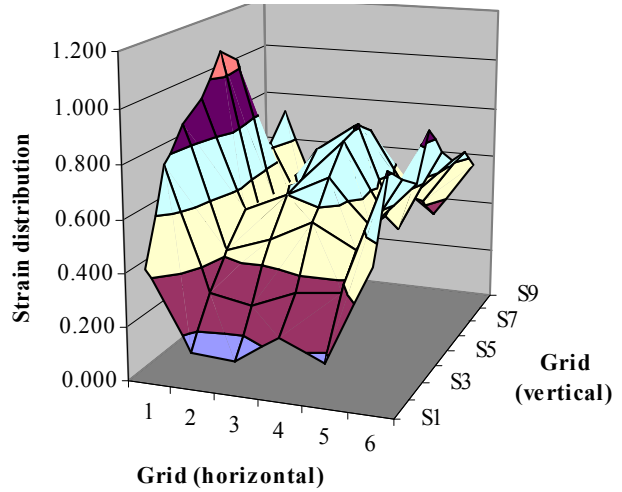

Fig. 9 Actual strain distribution pattern observed due to deformation of grid at the end of Stage 5

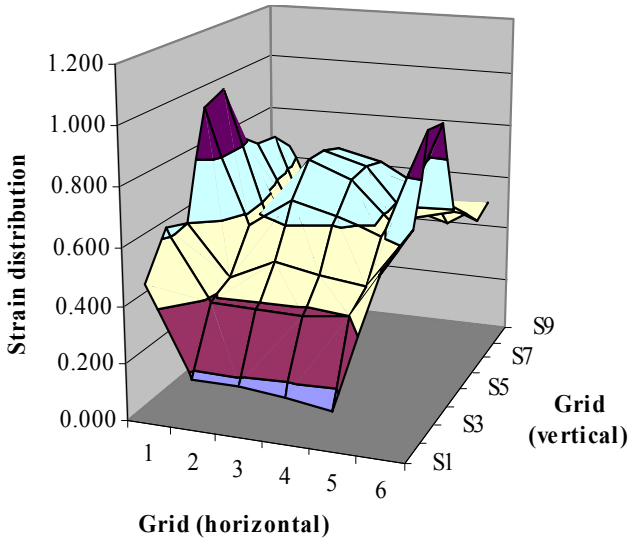

Fig. 10 Actual strain distribution pattern observed due to deformation of grid at the end of Stage 6

Figs. 5-10 depict the graph of actual strain distribution observed in the grids along the vertical direction and horizontal direction for the billet having H/D ratio as 1.9 for the flash thickness of 5 mm. This graphical representation helps in knowing the change in the strain distribution pattern as the deformation proceeds in the closed die forging.

VI. Conclusion

Finally, through this research work of analytical computations, simulation, and experimentation by using model material to study the closed die forging process, it may be concluded that the successful implementation of the simulation technique and experimental investigation by using the model material technique would depend upon the following:

- Primarily, the accuracy of the simulation and experimental investigation by using a model material technique is governed by the parameters such as the H/D ratio, strain rate, the flow of material in the die cavity, and strain hardening property of the actual material.
- It is very much essential that the frictional conditions between Die-Billet interface during the actual deformation process and the simulation are required to be nearly same; otherwise, significant deviations would be found in the results.
- The accurate selection of parameters is related to the material properties from the material property database which should match with the actual metallic material. If the resultant values contain percentage error more than 10% then the material properties are required to be obtained by testing the material using appropriate method.

However, the forging operations are very complex, the manufacturing by forging process still depends on the trial runs which tend to increase the lead-time. But, an integrated approach of forging simulation and optimization could significantly reduce the overall processing time for the components which are essentially manufactured by using the closed die forging process to achieve better material properties.

Nomenclature

C	Strain hardening constant
H	Initial height of billet
L	Die diameter
m	Strain rate sensitivity exponent
t	Deformation time
v	Ram speed
w	Flash width
β	Shear plane angle
ε	Strain before flash formation
θ	Time in seconds
λ	Thermal conductivity of the billet material
ρ	Density of the material
C_P	Specific heat of the material
D_o	Initial diameter of billet
F_I	Force required before flash formation
F_{II}	Force required after flash formation
T_B	Current billet temperature
T_D	Current die temperature
T_{BO}	Initial billet temperature
T_{DO}	Initial die temperature
T_{Bd}	Temperature rise of the billet due to deformation
ΔT	Increase of temperature due to deformation
t_{cont}	Time of contact or start of flash formation
t_i	Initial distance between flash lands of two die halves
$\bar{h}$	Current height of billet
$\bar{h}_c$	Average height of shearing zone at the beginning of flash formation
$\bar{h}_1$	Current average height of shearing zone
$\bar{t}$	Flash thickness
$\bar{t}_c$	Flash Thickness at the beginning of flash formation
α_T	Heat transfer co-efficient between die and billet
ε_1	Strain for zone 1
ε_3	Strain for zone 3
ε_4	Strain for zone 4
ε_{tc}	Strain at the beginning of the flash formation
μ_1	Coefficient of friction between die and billet

μ_2 Coefficient of shearing friction
σ_f Flow stress
σ_{max1} Maximum stress before flash formation
σ_{max2} Maximum stress after flash formation
$\dot{\varepsilon}$ Strain rate before flash formation
$\dot{\varepsilon}_1$ Strain rate for zone 1
$\dot{\varepsilon}_3$ Strain rate for zone 3
$\dot{\varepsilon}_4$ Strain rate for zone 4

In Fig. 3, encircled digits 1, 2, 3, and 4 depicts the respective zones.

REFERENCES

[1] Alexandre Polozine and Lirio Schaeffer, 2008, "Influence of the inaccuracy of thermal contact conductance coefficient on the weighted-mean temperature calculated for a forged blank", *Journal of materials processing technology*, 195, pp. 260–266.
[2] Altan T. and Boulger F. W., 1973, "Flow stress of metals and it's application in metal forming analysis", *Trans. ASME, Series B,* Vol. 95, pp. 1009-1018.
[3] B. Tomov, R. Radev, and V. Gagov, 2004, "Influence of flash design upon process parameters of hot die forging", *Journal of Materials Processing Technology*, 157-158, pp. 620–623.
[4] Biner S. B., 1992, "A procedure for determination of the strain distribution during simulation of metal forming using model material techniques", *Journal of Engineering for Industry*, Vol. 114, pp. 94-99.
[5] Boër C. R., Rebelo N., Rydstad H., and Schröder G., 1986, "Process Modeling of Metal Forming and Thermo-mechanical Treatment", Springer - Verlag, Berlin, Heidelberg.
[6] H. Grass, C. Krempaszky, and E. Werner, 2006, "3-D FEM-simulation of hot forming processes for the production of a connecting rod", *Computational Materials Science*, 36, pp. 480–489.
[7] H. Ou, J. Lan, C.G. Armstrong, and M.A. Price, 2004, "An FE simulation and optimisation approach for the forging of aeroengine components", *Journal of Materials Processing Technology*, 151, pp. 208–216.
[8] Hyunkee Kim, Kevin Sweeney, and Taylan Altan, 1994, "Application of computer aided simulation to investigate metal flow in selected forging operations", *Journal of Materials Processing Technology*, 46, pp. 127-154.
[9] M. Bakhshi-jooybari, I. Pillinger, P. P. Hartley, and T. A. Dean, 1996, "Finite element simulation and experimental study of hot closed-die upsetting", *International Journal of Machine Tools Manufacturing*, Vol. 36, No. 9, pp. 1021-1032.
[10] Markus Knoerr, Joon Lee, and Taylan Altan, 1992, "Application of the 2D finite element method to simulation of various forming processes", *Journal of Materials Processing Technology*, 33, pp. 31-55.
[11] Mielnik E.M., 1991, *Metal working Science and Engineering*, Mc-Graw Hill, Inc.
[12] Rusinoff S. E., 1959, *Forging and Forming Metals*, American Technical Society, Chicago, USA.
[13] Shinichiro Fujikawa, 2000, "Application of CAE for hot-forging of automotive components", *Journal of Materials Processing Technology*, 98 pp. 176-181.
[14] Thomsen E. G., Yang C.T., and Kobayashi S., 1965, *Mechanics of Plastic Deformation in Metal Processing*, Mc - Millan Co., New York.
[15] William R.D. Wilson, Steven R. Schmid, and Jiying Liu, 2004, "Advanced simulations for hot forging: heat transfer model for use with the finite element method", *Journal of Materials Processing Technology*, 155–156, pp. 1912–1917.